

Singular motions of asymmetric rotators*

William G. Harter

Instituto de Física, Departamento de Eletrônica Quântica, Universidade Estadual de Campinas, Campinas, São Paulo, Brasil

Chong C. Kim

Department of Physics, University of Southern California, University Park, Los Angeles, California 90007
(Received 9 December 1975; revised 24 February 1976)

An apparatus is described that shows clearly and quantitatively the spectacular motion of free rotating rigid and semirigid bodies moving near their inertial singularities. A geometric construction is shown that makes the theory of this motion clear.

I. INTRODUCTION

Determining the motion of a freely rotating body is one of the most beautiful classical mechanics problems. The solutions found by Euler, Poinot, Routh, and others are given in most modern advanced texts.^{1,2}

However, there is still some difficulty in exhibiting the mathematical solutions and producing clear demonstrations of them. The standard demonstration of a flipping tennis racquet is completed so quickly that it appears to be a trick (we assume that Skylab is not available for the experiment), and the usual mathematical description involving the angular velocity ellipsoid is more obscure than it needs to be.

We describe a simple air support apparatus that provides a spectacular and clear demonstration of the peculiar singular motions of an asymmetric rigid body. We show a geometric construction involving a combination of the ellipsoids of angular velocity and angular momentum, through which the motion may be understood more easily. We use this to show how another type of peculiar motion can occur for a semirigid body, and explain how this may be demonstrated also.

$$\begin{pmatrix} L_x \\ L_y \\ L_z \end{pmatrix} = \sum_j m_j \begin{pmatrix} y_j^2 + z_j^2 & -x_j y_j & -x_j z_j \\ -y_j x_j & x_j^2 + z_j^2 & -y_j z_j \\ -z_j x_j & -z_j y_j & x_j^2 + y_j^2 \end{pmatrix} \begin{pmatrix} \omega_x \\ \omega_y \\ \omega_z \end{pmatrix} \quad (3)$$

Similarly, the kinetic energy E of the body is expressed conveniently in terms of this inertia operator, and the angular velocity vector:

$$\begin{aligned} E &= (1/2) \sum_j m_j \dot{\mathbf{r}}_j \cdot \dot{\mathbf{r}}_j = (1/2) \sum_j m_j (\boldsymbol{\omega} \times \mathbf{r}_j) \cdot (\boldsymbol{\omega} \times \mathbf{r}_j) \\ &= (1/2) \sum_j m_j \{ \boldsymbol{\omega} \cdot [\mathbf{r}_j \times (\boldsymbol{\omega} \times \mathbf{r}_j)] \} = (1/2) \boldsymbol{\omega} \cdot \mathbf{I} \cdot \boldsymbol{\omega}. \quad (4) \end{aligned}$$

A convenient geometrical visualization of these equations is due originally to Poinot. There exists a coordinate system (labeled as the principal body axes 1, 2, and 3) in which \mathbf{I} is diagonal and the kinetic-energy relation [Eq. (4)] becomes the standard equation of an ellipsoid.

$$\begin{aligned} E &= (1/2) \boldsymbol{\omega} \cdot \mathbf{I} \cdot \boldsymbol{\omega} = (1/2) |\omega_1 \ \omega_2 \ \omega_3| \begin{vmatrix} I_1 & 0 & 0 \\ 0 & I_2 & 0 \\ 0 & 0 & I_3 \end{vmatrix} \begin{pmatrix} \omega_1 \\ \omega_2 \\ \omega_3 \end{pmatrix} \\ &= (1/2) (I_1 \omega_1^2 + I_2 \omega_2^2 + I_3 \omega_3^2), \\ 1 &= \omega_1^2/a_1^2 + \omega_2^2/a_2^2 + \omega_3^2/a_3^2, \quad a_j = (2E/I_j)^{1/2}. \quad (5) \end{aligned}$$

The modifications of existing theory and experiments which we describe do not represent a great change. (Air-supported symmetric tops have been commercially available for some years.) However, we find that the modifications are well worth the little extra effort which they require.

II. REVIEW OF ROTATION THEORY

The standard vector definition of angular velocity $\boldsymbol{\omega}$ and angular momentum \mathbf{L} for a rigid body of mass points m_j at positions \mathbf{r}_j gives the following relations between them:

$$\begin{aligned} \mathbf{L} &= \sum_j \mathbf{r}_j \times (m_j \dot{\mathbf{r}}_j) = \sum_j \mathbf{r}_j \times (m_j \boldsymbol{\omega} \times \mathbf{r}_j), \\ \mathbf{L} &= \sum_j m_j [(\mathbf{r}_j \cdot \mathbf{r}_j) \boldsymbol{\omega} - \mathbf{r}_j (\mathbf{r}_j \cdot \boldsymbol{\omega})]. \quad (1) \end{aligned}$$

As described in many texts, this relation between \mathbf{L} and $\boldsymbol{\omega}$ is concisely expressed by the operation of the inertia tensor \mathbf{I} :

$$\mathbf{L} = \mathbf{I} \cdot \boldsymbol{\omega}, \quad \mathbf{I} = \sum_j m_j [(\mathbf{r}_j \cdot \mathbf{r}_j) \mathbf{I} - \mathbf{r}_j \mathbf{r}_j] \quad (2)$$

or by a matrix representation of \mathbf{I} :

Given that E is conserved, Eq. (5) demands that the terminus of vector $\boldsymbol{\omega}$ lie on this ellipsoid, and this, in combi-

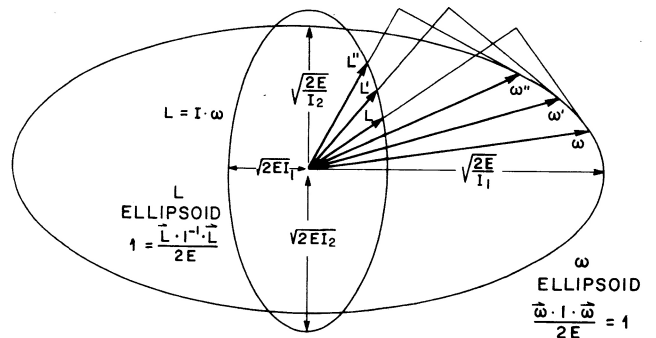
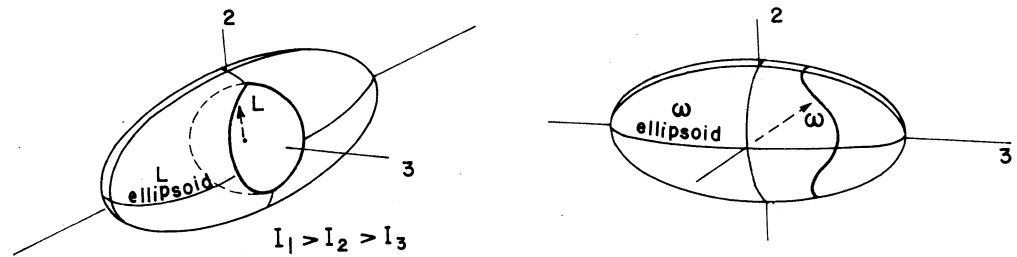


Fig. 1. Geometry of tensors. The inertia tensors \mathbf{I} and \mathbf{I}^{-1} define the $\boldsymbol{\omega}$ and \mathbf{L} ellipsoids respectively. For each vector $\boldsymbol{\omega}$ on the $\boldsymbol{\omega}$ ellipsoid, there is a vector $\mathbf{L} = \mathbf{I} \cdot \boldsymbol{\omega}$ on the \mathbf{L} ellipsoid as sketched in the figure. \mathbf{L} is normal to the tangent plane at $\boldsymbol{\omega}$ and vice versa.

Fig. 2. Constraints of motion. The L vector is constrained by energy and momentum conservation to be at the intersection of a sphere and the L ellipsoid in the body coordinate system. The constraint on L is then transformed into a constraint on ω .



nation with Eq. (2), restricts vector L to another ellipsoid defined by

$$E = (1/2) \mathbf{L} \cdot \mathbf{I}^{-1} \cdot \mathbf{L}$$

$$= (1/2) |L_1 \ L_2 \ L_3| \begin{vmatrix} I_1^{-1} & 0 & 0 \\ 0 & I_2^{-1} & 0 \\ 0 & 0 & I_3^{-1} \end{vmatrix} \begin{vmatrix} L_1 \\ L_2 \\ L_3 \end{vmatrix}$$

$$= (1/2) (L_1^2/I_1 + L_2^2/I_2 + L_3^2/I_3),$$

$$1 = L_1^2/A_1^2 + L_2^2/A_2^2 + L_3^2/A_3^2,$$

$$A_j = (2EI_j)^{1/2}. \quad (6)$$

Now it is easy to visualize the relation between vectors ω and L at any instant. L is along the normal to the plane tangent to the ω ellipsoid [Eq. (5)] at ω , and ω is along the normal to the plane tangent to the L ellipsoid [Eq. (6)] at L . A two-dimensional sketch of this is given in Fig. 1. (This construction is valid for any positive definite operators. Treatment of other operators lends itself to similar constructions involving hyperboloids.)

Now if no torques are applied to the spinning body, then its L vector must keep a constant direction in the laboratory (x, y, z) coordinate frame, and a constant length in all co-origial coordinate systems including the body axes (1,2,3). The latter constraint restricts vector L to the line of intersection between the L ellipsoid and a sphere of radius $|L|$, and as shown in Fig. 2, this constrains the body axis motion of vector ω to some curve (called a polhode) on the ω ellipsoid. A family of polhodes shown in Fig. 3 are produced by trying various values $|L|$ with E held constant.

The spatial or laboratory constraints and the energy equations [Eqs. (5) and (6)] together demand that the plane normal to L (and tangent to the ω ellipsoid) be fixed in space at a constant distance from body center:

$$\omega \cdot \mathbf{I} \cdot \omega = \omega \cdot \mathbf{L} = 2E. \quad (7)$$

All this leaves the ω ellipsoid to roll around between two parallel space fixed planes as shown in Fig. 4. Since ω always defines the point of tangency, the ω ellipsoid rolls

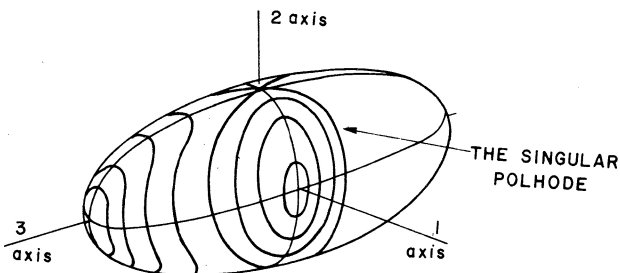


Fig. 3. Polhodes. A family of constraint curves for the vector ω in the body system, or "polhodes," are separated into two distinct groups by a curve called the singular polhode.

without slipping. Indeed, if one were to fashion an ellipsoid of iron stuck between two parallel magnetic pole faces, an analog of the motion would result. (It is interesting to show that an asymmetric solid homogeneous elliptical body could never be its own inertial ω ellipsoid, so the mathematical model requires some static friction for it to move "correctly.")

III. DEMONSTRATION APPARATUS

In order to demonstrate the peculiarities of the rigid body motion with a physical model, we put brass pins and bolts in billiard balls and floated them on air bearing supports (Fig. 5). Some of the most spectacular effects occur when the moments of inertia are all different ($I_1 < I_2 < I_3$) but not very different. An arrangement that accomplishes this is shown in Fig. 5.

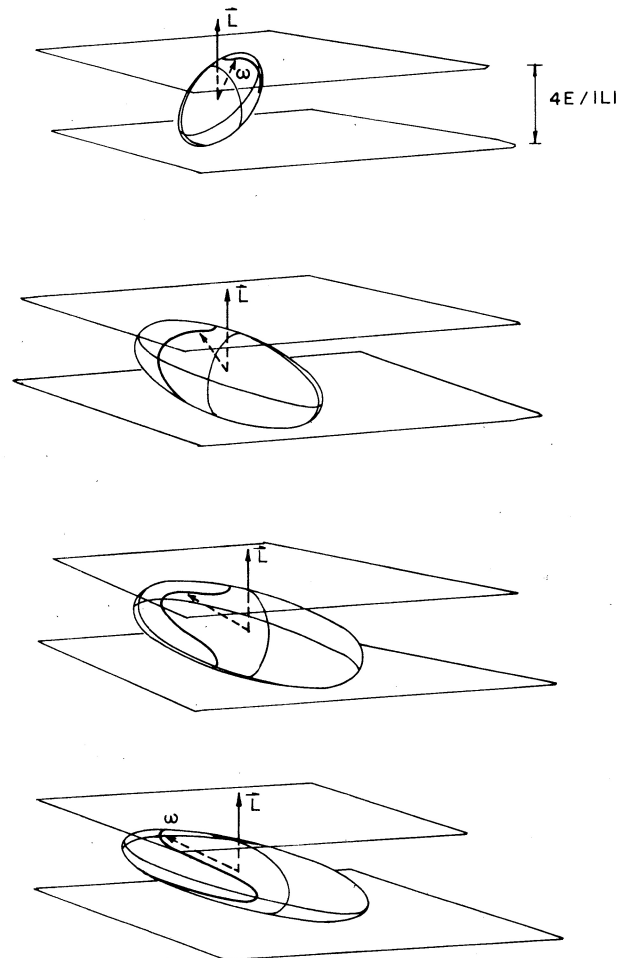


Fig. 4. Model of rotational motion near the singular polhode.

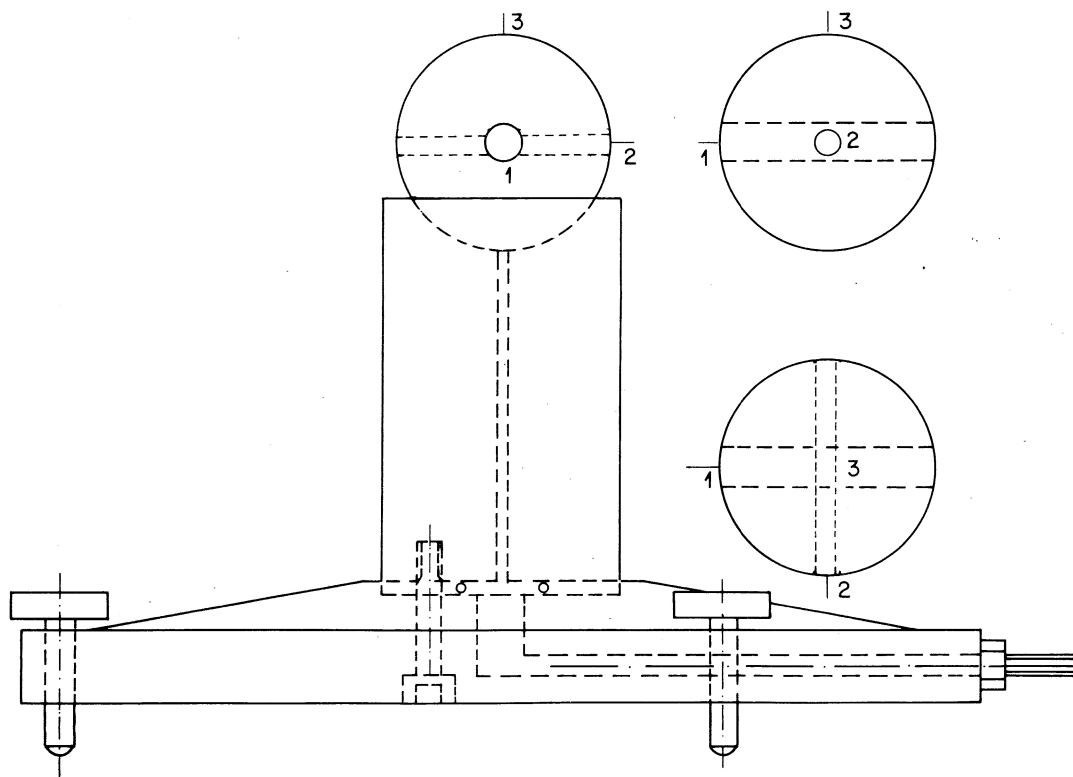


Fig. 5. Demonstration apparatus. *Rigid body experiment.* Machined aluminum base is bolted to Plexiglas column with ring seal between the connecting air passages. Billiard ball containing two orthogonal press-fit brass rods rides on a cushion of air provided by a pressure source. (Less than 2 psi pressure is needed if the ball is balanced and the pocket fits it well.) When each brass rod is turned, a small (No. 70–80) hole should be drilled into the center of either end to serve as receptacles for a pin point. The ball can be started rotating by hand precisely on the desired axis using the pin point as an initial bearing. Spectacular reversals occur when the 2 axis is tried. The 1 and 3 axes are stable. *Semirigid body experiment.* The same construction is made except that a balanced, 1½- to 1¾-in.-long segment is cut out of the 1-axis brass rod leaving a cylindrical cavity inside the ball. Mercury can be injected through a pinhole in one rod end while trapped air escapes at the opposite end until the cavity is completely full, and the holes may then be sealed. Because the fluid may dissipate energy, only the 3 axis is a stable rotation axis.

Plastic billiard balls are the least expensive round and balanced objects we found readily available. They are comparatively easy to machine on a lathe and can be filled with various balanced masses, magnets, liquids, springs, or whatever one finds to be potentially instructive.

The simple model shown in Fig. 5 has the moments of inertia given approximately by

$$I_1 = (2M/5 + m_2/3)R^2 + m_1r_1^2/2 + m_2r_2^2/4,$$

$$I_2 = (2M/5 + m_1/3)R^2 + m_2r_2^2/2 + m_1r_1^2/4, \quad (8)$$

$$I_3 = (2M/5 + m_1/3 + m_2/3)R^2 + m_1r_1^2/4 + m_2r_2^2/4,$$

where m_1 and m_2 are the masses of the two transverse metal bolts, less the mass of corresponding equal volumes of plastic, and r_1 and r_2 are their radii. (We ignore the extra inertia due to counting the bolt intersection twice, and that which is lost by filling the ends to conform to the sphere.)

The balls we used had radius $R = 2\frac{1}{4}$ in. and mass $M = 115$ g. The rotator with the longest time constant (see Sec. IV) had bolts of radii $r_1 = \frac{1}{4}$ in. and $r_2 = \frac{1}{16}$ in. made of brass having a density of 8.40 g/cm³. The inertia values obtained are $I_1 = 396$ g cm², $I_2 = 524$ g cm², and $I_3 = 533$ g cm².

Now, if the initial rotation axis $\omega(0) \equiv \mathbf{W}$ is set on or near the +2 axis or anywhere on or near the so-called singular polhode of Fig. 3, an extraordinary rotation results. The top will appear to rotate smoothly for some time (this time interval is calculated in Sec. IV), after which it will suddenly

reverse itself to settle the -2 axis for a similar length of time, followed by reversal, rotation, reversal, etc. One may set whatever initial axis is desired with some accuracy by drilling tiny pin pockets at select points on the surface of the ball or into the brass rods near the 2 axis. The results of various initial conditions are discussed below.

A very interesting effect can occur when a rotator such as the one in Fig. 5 is loaded along one axis with a fluid such as mercury. Supposing again that the three principal inertia satisfy $I_1 < I_2 < I_3$, we would expect for a rigid body that axes 1 and 3 were stable while 2 behaved extraordinarily. However, with energy dissipation through the fluid occurring, we find that an initial ω that points near the 1 axis will, if not perfectly centered, move away from that axis, pass quickly through the vicinity of the 2 axis, and settle finally into the 3 axis where it will remain. One can see that this catastrophic overturning must occur because E decreases while L , assuming no external torques, remains a constant vector. The L ellipse in Fig. 2, shrinks until it just fits inside the L sphere. Indeed, the "ground state" value for E is $|L|^2/2I_3$. The dissipating fluid will be rotating rigidly at this point and no further energy can be lost. This upsetting effect brought the untimely end to the useful life of a satellite several years ago.³

In either of the experiments described here, it is interesting to put a dot of fluorescent paint on the initial axis, and illuminate the moving ball with an uv lamp. A time exposure photograph of one reversal shows a logarithmic spiral.

IV. CALCULATING TIME BETWEEN REVERSALS

If one could adjust the initial ω vector to be exactly on the 2 axis, a rigid freely rotating body with $I_1 < I_2 < I_3$ would remain in uniform rotation about the axis forever. However, any deviation or disturbance would precipitate an overturning. We now see how long it takes this body to overturn when the initial ω makes a small angle ϵ with the 2 axis.

The Euler equation for the motion of the rigid body is given by

$$\dot{\mathbf{L}} = \boldsymbol{\omega} \times \mathbf{L}, \quad (9)$$

which takes the following form for the 2 component:

$$\dot{\omega}_2 + \omega_1 \omega_3 (I_1 - I_3) / I_2 = 0. \quad (10)$$

Solving Eq. (10) for $\omega \equiv \omega_2$ using Eqs. (5) and (6), we obtain the following:

$$\dot{\omega} = (a - b\omega^2)^{1/2} (c - d\omega^2)^{1/2} / I_2 (I_1 I_3)^{1/2}, \quad (11)$$

where the constants $a-d$ [Eq. (12)] depend on initial conditions and the inertial moments as follows:

$$\begin{aligned} a &= 2EI_3 - L^2, & b &= I_2(I_3 - I_2), \\ c &= L^2 - 2EI_1, & d &= I_2(I_2 - I_1), \\ a &= I_2(I_3 - I_2)W^2 \cos^2 \epsilon, \end{aligned}$$

$$c = [I_2(I_2 - I_1) \cos^2 \epsilon + I_3(I_3 - I_1) \sin^2 \epsilon] W^2, \quad (12)$$

where we have assumed initial conditions

$$\omega_1(0) = 0, \quad \omega_2(0) = W \cos \epsilon, \quad \omega_3(0) = W \sin \epsilon. \quad (13)$$

Equation (11) is that of an elliptic function as given by

$$\begin{aligned} t &= \left(\frac{I_1 I_2 I_3}{(I_3 - I_2)(L^2 - 2EI_1)} \right)^{1/2} \\ &\times \int_0^{\Omega'} \frac{d\Omega}{(1 - \Omega^2)^{1/2} (1 - k^2 \Omega^2)^{1/2}}, \quad (14) \end{aligned}$$

where the following substitutions were made:

$$k = (ad/bc)^{1/2}, \quad \omega = (a/b)^{1/2} \Omega = \Omega W \cos \epsilon. \quad (15)$$

A further substitution $\Omega = \sin \phi$ reduces the integral in Eq. (14) to the following customary form of the elliptic function:

$$\begin{aligned} \int_0^{\Omega'} \frac{d\Omega}{(1 - \Omega^2)^{1/2} (1 - k^2 \Omega^2)^{1/2}} \\ = \int_0^{\phi'} \frac{d\phi}{(1 - k^2 \sin^2 \phi)^{1/2}} \equiv \text{sn}^{-1}(\phi', k). \quad (16) \end{aligned}$$

Equation (16) gives the quarter-cycle period if the integration limit is set to unity, $\Omega' = 1$, which is equivalent to setting $\phi' = \pi/2$ in Eq. (16). The latter integral is tabulated commonly.

Using Eqs. (12), (14), and (16), we obtain the following equation for a half-cycle period, i.e., the time for one reversal:

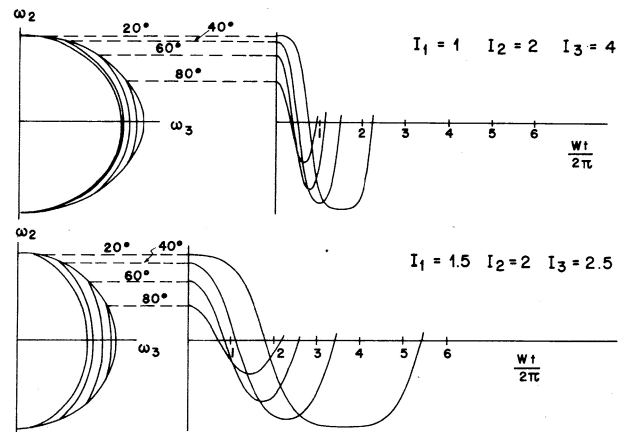


Fig. 6. Exact solutions. The motion of the ω vector for an asymmetric and a not-so-asymmetric body are compared. Various polhodes are shown on the left-hand side while the corresponding time behavior is plotted on the right-hand side.

$$\begin{aligned} t &= \frac{2}{W} \\ &\times \left(\frac{I_1 I_2 I_3}{(I_3 - I_2)[I_2(I_2 - I_1) \cos^2 \epsilon + I_3(I_3 - I_1) \sin^2 \epsilon]} \right)^{1/2} \\ &\times \text{sn}^{-1} \left(\frac{\pi}{2}, k \right), \quad (17a) \end{aligned}$$

$$t \rightarrow \frac{2}{W} \left(\frac{I_1 I_2}{(I_3 - I_2)(I_2 - I_1)} \right)^{1/2} \text{sn}^{-1} \left(\frac{\pi}{2}, k \right), \quad (17b)$$

where

$$k = \left(\frac{I_2(I_2 - I_1)}{I_2(I_2 - I_1) \cos^2 \epsilon + I_3(I_3 - I_1) \sin^2 \epsilon} \right)^{1/2} \cos \epsilon, \quad (18a)$$

$$k \rightarrow 1 - (I_3/I_2)[(I_3 - I_1)/(I_2 - I_1)](\epsilon^2/2). \quad (18b)$$

The limiting forms [Eqs. (17) and (18b)] become good approximations for $\epsilon < 10^\circ$. The approximate number of revolutions accomplished by a body before it overturns is given by the product of $W/2\pi$, the number of revolutions per second, and the right-hand side of Eq. (17b). Exact solutions for various I_j and ϵ are displayed in Fig. 6.

If one desires to increase the reversal time, it should be done through the first factor in Eq. (17b). The integral in the second factor is usually only as large as 7 or 8 in our experiments ($\epsilon = 10^\circ$ gives 3.1, $\epsilon = 1^\circ$ gives 5.4, and $\epsilon = 0^\circ$ gives 9.5). This is a good demonstration of the behavior of an elliptic function near its singularity.

*Work supported in part by a grant by Centro Technico Aeroespacial, S.P., Brazil.

¹H. Goldstein, *Classical Mechanics* (Addison-Wesley, Reading, MA, 1965).

²K. Symon, *Mechanics* (Addison-Wesley, Reading, MA, 1971).

³R. Edwards (private communication).